Adaptive absorbing boundary conditions for Schrödinger-type equations: application to nonlinear and multi-dimensional problems

Zhenli Xu[1], Houde Han[1,2], Xiaonan Wu[3]

1. Department of Mathematics, University of Science and Technology of China, Hefei, 230026, China. Email: xuzl@ustc.edu

2. Department of Mathematical Sciences, Tsinghua University, Beijing, 100084, China. E-mail: hhan@math.tsinghua.edu.cn

3. Department of Mathematics, Hong Kong Baptist University, Kowloon, Hong Kong, China. Email: xwu@hkbu.edu.hk

Abstract

We propose an adaptive approach in picking the wave-number parameter of absorbing boundary conditions for Schrödinger-type equations. Based on the Gabor transform which captures local frequency information in the vicinity of artificial boundaries, the parameter is determined by an energy-weighted method and yields a quasi-optimal absorbing boundary conditions. It is shown that this approach can minimize reflected waves even when the wave function is composed of waves with different group velocities. We also extend the split local absorbing boundary (SLAB) method [Z. Xu and H. Han, *Phys. Rev. E*, 74(2006), pp. 037704] to problems in multidimensional nonlinear cases by coupling the adaptive approach. Numerical examples of nonlinear Schrödinger equations in one- and two dimensions are presented to demonstrate the properties of the discussed absorbing boundary conditions.

Key words: Nonlinear Schrödinger equations, artificial boundary conditions, time-splitting, finite difference method, Fourier transform, group velocity

1 Introduction

The numerical solution of partial differential equations on unbounded domains arises in a large variety of applications in science and engineering. A typical example we concern in this paper is the nonlinear Schrödinger-type equations in multi-dimensional space, which describe the gravity waves on deep water in fluid dynamics, the pulse propagations in optics fibers, and Bose-Einstein

condensations in very low temperature; see Sulem and Sulem [1] and Agrawal [2] for details.

One principal difficulty to obtain numerical solutions of these problems is the unboundedness of the physical domain. In order to overcome this difficulty, the artificial boundary method [3–6] has been widely studied in recent decades, with which the original problem is reduced to an approximate (or equivalent) problem in a truncated computational domain. The key point of the artificial boundary method is to construct a "suitable" artificial boundary condition on the given artificial boundary for the problem. In particular, when we consider problems containing wave propagations, we hope the artificial boundary conditions can annihilate all the incident waves so as that there is no or minor reflected waves propagating into the interior domain. These artificial boundary conditions are also known as absorbing boundary conditions. For linear problems, many strategies have been developed to obtain accurate and efficient boundary conditions, such as [7, 8] for hyperbolic wave equations, [9, 10] for elliptic equations, and [11, 12] for parabolic equations. In the case of the linear Schrödinger equation, there are also several works [13–19] developing transparent boundary conditions and studying their difference approximations and stability. They utilized the integral transform (Laplace or Fourier transform) or series expansion method to construct accurate boundary conditions which are in nonlocal forms. In practical applications the fast evaluation method [20] must be developed to discretize the nonlocal boundary conditions. On the other hand, the authors in [21–26] constructed absorbing boundary conditions by deriving polynomial approximations to nonlocal operators in transparent boundary conditions with Taylor or rational expansions. This class of boundary conditions is local, and hence they are easy to implement.

The treatment of the boundary conditions on the artificial boundary for nonlinear equations is difficult in general. Hagstrom and Keller [27] studied some nonlinear elliptic problems by linearizing the equations. Han et al. [28] and Xu et al. [29] respectively discussed the nonlinear Burgers eqquation and Kardar-Parisi-Zhang equation. The exact nonlinear artificial conditions have been obtained by using the Cole-Hopf transformation. For the works related with the nonlinear Schrödinger equations under consideration, Zheng [30] obtained the transparent boundary condition using the inverse scattering transform approach for the cubic nonlinear Schrödinger equation in one dimension. Antonie et al. [31] also studied the one-dimensional cubic nonlinear Schrödinger equation and constructed several nonlinear integro-differential artificial boundary conditions. In [32, 33], Szeftel designed absorbing boundary conditions for one-dimensional nonlinear wave equation by the potential and the paralinear strategies. Especially, the one-dimensional nonlinear Schrödinger equation was discussed. The perfectly matched layer (PML) [34] was also applied to handling the nonlinear Schrödinger equations in which the nonlinear term can be general.

Recently, Xu and Han [35] proposed a split local absorbing boundary (SLAB) method through a time-splitting procedure to design absorbing boundary conditions for one-dimensional nonlinear Schrödinger equations. The local absorbing boundary conditions were imposed on the split linear subproblem and yielded a full scheme by coupling the discretizations for the interior equation and boundary subproblems. In using local boundary conditions for the Schrödinger-type equations, it is important to pre-estimate a wave-number parameter (or the group velocity parameter) of the wave function, as is illustrated in [35], which strongly influences the accuracy of the boundary condition. In this paper, we present an adaptive parameter selection approach based on the Gabor transform [36] to capture the wave number near the artificial boundaries in order that the constructed absorbing boundary conditions can minimize the reflected wave. In particular, for nonlinear problems, a wave packet of the nonlinear Schrödinger equation will evolve into various wave packets with different wave numbers. With the Gabor transform, the boundary conditions can succeed in reflecting the local structure of the frequency context of the wave. Particular focus of this paper is to apply the adaptive approach to multi-dimensional problems with nonlinear terms, in which very few boundary conditions can work well.

The organization of this paper is the following. In section 2, we first give a brief overview of absorbing boundary conditions for the linear Schrödinger equation, and then discuss the adaptive strategy in picking the parameter in boundary conditions. Two-dimensional boundary conditions for linear problems are also proposed in this section. In section 3, we are devoted to the two-dimensional nonlinear Schrödinger equation and its numerical issues in both interior domain and artificial boundaries. Numerical examples are investigated in section 4.

2   Absorbing boundary conditions for the linear Schrödinger equation

2.1   Brief overview of the absorbing boundary conditions

We shall give a brief overview for local absorbing boundary conditions of the linear Schrödinger equation in one dimension

$$i\psi_t = -\psi_{xx} + V\psi, \quad x \in \mathbb{R}, \ t > 0. \tag{1}$$

Set the truncated subdomain $\Omega_i = [x_l, x_r]$ be the computational domain. Suppose that the potential $V(x)$ is constant in the exterior domain $\Omega_e = (-\infty, x_l] \cup [x_r, +\infty)$.

Consider the solutions of the Schrödinger wave equation (1) in the form of one Fourier mode:

$$\psi(x,t) = e^{-i(\omega t - kx)}, \tag{2}$$

where k is the wave number corresponding to space x, and ω is the time frequency. We have the dual relation between the space-time (x,t) domain and the wave number-frequency (k,ω) domain: $k \leftrightarrow -i\frac{\partial}{\partial x}$, and $\omega \leftrightarrow i\frac{\partial}{\partial t}$. Using this duality, we can transform Schrödinger wave equation (1) into the Fourier domain resulting in a dispersion relation to the equation:

$$k^2 = \omega - V. \tag{3}$$

Under the framework of Engquist and Majda approach [7], solving (3) in terms of the wave number k gives

$$k = \pm\sqrt{\omega - V}, \tag{4}$$

where the plus sign corresponds to waves moving to the positive x direction, while the minus sign indicates wave motions in opposite direction. The exact transformation of (4) to physical space is nonlocal in time so that one has to save all history data in memory in order to perform numerical calculations. An effective substitution is to approximate the square root through a rational polynomial.

Let us consider the right exterior domain and obtain boundary condition at $x = x_r$; that is, the plus sign is taken in (4). Similar procedure can be performed in the left exterior domain. As in [25], we denote the absorbing boundary condition by ABC(j_1, j_2) for that using (j_1, j_2)-Padé approximation, where j_1, j_2 are the degrees of the polynomials in the numerator and denominator, respectively.

The first absorbing boundary condition is the one developed in Shibata [21]. The author used a linear interpolation to approximate the square root in (4) through imposing two adjustable parameters which were positive and called the kinetic energy parameters related to the group velocities of the wave function [24], that is,

$$\sqrt{\omega - V} = \frac{1}{\alpha_1 + \alpha_2}(\omega - V) + \frac{\alpha_1\alpha_2}{\alpha_1 + \alpha_2}. \tag{5}$$

Then using the dual relations to transform back into physical space yields an absorbing boundary condition

$$i(\alpha_1 + \alpha_2)\psi_x + (i\psi_t - V\psi + \alpha_1\alpha_2\psi) = 0. \tag{6}$$

Kuska [22] used a $(1, 1)$-Padé approximation to k^2 centered at a positive con-

stant $k = k_0$

$$k^2 = k_0^2 \frac{-3k + k_0}{k - 3k_0} + O((k - k_0)^3), \tag{7}$$

and then obtained a second absorbing boundary condition ABC(1,1),

$$-\psi_{xt} + i(3k_0^2 - V)\psi_x + (k_0^3 - 3k_0 V)\psi + i3k_0\psi_t = 0 \tag{8}$$

after transforming back into physical space through the dual transform. Here the range of validity of the Padé polynomial is the positive part $k > 0$. Alonso-Mallo and Reguera [25] developed a class of absorbing boundary conditions including ABC(2,1), ABC(3,2) and ABC(2,0) and absorbing boundary conditions discussed above. Fevens and Jiang [24] developed a distinct method to construct absorbing boundary conditions. The authors used the group velocity $C = \frac{\partial \omega}{\partial k} = 2k$ to design a differential equation as absorbing boundary condition, which can absorb waves with certain group velocities C_l, $l = 1, \cdots, p$,

$$\prod_{l=1}^{p} \left(i\partial_x + \frac{C_l}{2} \right) \psi = 0. \tag{9}$$

If we substitute the temporal derivative into ABC(1,0) with the original equation $i\psi_t = -\psi_{xx} + V\psi$, then we obtain

$$(i\partial_x + \alpha_1)(i\partial_x + \alpha_2)\psi = 0. \tag{10}$$

It is a special case of Fevens and Jiang's formula (9) with $C_1 = 2\alpha_1$ and $C_2 = 2\alpha_2$. We use the original equation again to replace the temporal derivative terms in (8) and get

$$\left(i\frac{\partial}{\partial x} + k_0 \right)^3 \psi = 0, \tag{11}$$

which is also a special case of Eq. (9) for $p = 3$ and group velocities $C_1 = C_2 = C_3 = 2k_0$.

2.2 Weighted wave-number parameter based on Gabor transform

In the above absorbing boundary conditions, the authors all imposed parameters in the formulae with different meanings. Therefore, perhaps one of the most important issues is how to pick suitable parameters such that they can minimize the reflection of the wave. Noticing that the relation between the group velocity C and wave number k is

$$C = \frac{\partial \omega}{\partial k} = 2k, \tag{12}$$

we need only calculate one of them.

For the initial wave composed of waves with different group velocities, they shall evolve into different wave packets. Each of them has an unchanged group velocity. These wave packets hit the artificial boundary separately. Therefore, in a general physical insight, if only we pre-estimate one component of group velocities which is a function of time, the boundary condition can well annihilate the reflected wave. Let us consider the third-order boundary condition ABC(1,1) given in section 2.1 as example to introduce our idea, in which only one parameter k_0 need to be pre-estimated. Similarly, for convenience, the discussion is focused on the right boundary.

It is important that we must estimate the parameter in the frequency domain. Note that the wave function at time t can be expressed in terms of a Fourier series and a single Fourier mode is essentially a plane wave. A general strategy suggested in Fevens and Jiang [24] to pick the wave-number parameter k_0, which is a function of time t, is to use a Fourier series expansion of the physical variable in space, and then take one of the positive components so that its Fourier mode is dominant. The Fourier transform presents the frequency information of the wave over the whole interior domain. However, in our situations to construct absorbing boundary conditions, we are interested in the frequency content of the wave in the vicinity of the artificial boundary. So it is necessary to obtain the local structure of the wave in the frequency domain. One approach is to replace the Fourier transform with the Gabor transform which is also known as a windowed Fourier transform. In the frequency domain with the Gabor transform, we have

$$\hat{\psi}(k,t) = \int_{x_l}^{x_r} W(x)\psi(x,t)e^{-ikx} = \int_{x_r-b}^{x_r} \psi(x,t)e^{-ikx}, \tag{13}$$

where the window function is

$$W(x) = \begin{cases} 1, & x \in [x_r - b, x_r], \\ 0, & \text{otherwise}, \end{cases} \tag{14}$$

and b is the window width. Then one choice for k_0 is take the frequency such that its spectrum is the maximum; that is,

$$|\hat{\psi}(k_0,t)| = \sup_{k \geq 0}\{|\hat{\psi}(k,t)|\}. \tag{15}$$

We remark that we can also utilize the time windowed Fourier transform to approximate temporal frequency information ω, and then obtain an estimation of the wave number k_0 with the dispersion relation (4). However, it is clear that the Gabor transform in time depends on the history data on the artificial boundaries. Therefore, although the formulae of absorbing boundary conditions are in local forms, they are nonlocal in practice.

The formula (15) is also not the best choice in many practical computations. On one hand, this procedure involves many logical "if" structures in order to compare the magnitudes of the Fourier modes, which are not very efficient in calculations in some computational environments. On the other hand, when two Fourier modes are both dominant, it is obvious to choose k_0 a medial value of two different wave numbers instead of taking one of them, in order to minimize the reflection. Therefore, an improvement is to use a weighted strategy, we call it the energy-weighted wave-number parameter selection approach, as follows,

$$k_0 = \int_0^\infty (|\hat{\psi}(k,t)|^p k) dk \bigg/ \int_0^\infty |\hat{\psi}(k,t)|^p, \tag{16}$$

with p a positive real number.

We give the following remarks:

Remark 1. The window width b is correlative with the Gibbs phenomena induced by the discontinuities of the window function. The narrower b is, the more Gibbs effect. However, if the window width b is very large, then the obtained parameter cannot correctly response the frequency information in the vicinity of the boundary.

Remark 2. When $p = +\infty$, the Eq. (16) is equivalent to (15). However, numerical experiments illustrate that the absorbing boundary conditions work best when p is in a suitable intermediate interval. Table 1 suggests $p = 4$ is a good choice.

2.3 Multi-dimensions

Let us consider the extension of previous ABCs which are local for the linear Schrödinger equation in two dimensions:

$$i\psi_t = -(\psi_{xx} + \psi_{yy}) + V\psi, \quad (x,\ y) \in \mathbb{R}^2, \tag{17}$$

with the potential V constant. Denote the dual variables to (x, y, t) by (ξ, η, ω) with the correspondence $\xi \leftrightarrow -i\frac{\partial}{\partial x}$, $\eta \leftrightarrow -i\frac{\partial}{\partial y}$, and $\omega \leftrightarrow i\frac{\partial}{\partial t}$. Then the related dispersion relation to Eq. (17) gives

$$\xi^2 + \eta^2 = \omega - V. \tag{18}$$

We truncate the unbounded domain to get a computational domain $[0\ ,L]^2$. Without loss of generality, consider the east boundary $\Gamma_e = \{(x,y)|x = L,\ 0 \leq y \leq L\}$ which corresponds to the positive branch to ξ of the dispersion relation (18) as follows,

$$\xi = \sqrt{\omega - V - \eta^2}. \tag{19}$$

With the same procedure as that used in one dimensional case, we can get the similar ABCs as in section 2.1. We consider the $(1,1)-$Padé approximation to the square ξ^2 in the dispersion relation centered as a positive constant $\xi = \xi_0$, and obtain an approximation to (19)

$$(\eta^2 - \omega + V - 3\xi_0^2)\xi + \xi_0^3 - 3\xi_0(\eta^2 - \omega + V) = 0, \qquad (20)$$

which is first order in ξ. Here the range of validity of the Padé polynomial is the positive part $\xi > 0$; see Kuska [22]. Transforming (20) back into the physical space through the dual relations, we have an ABC on the right boundary of the form:

$$\Gamma_e : \quad i\psi_{xyy} - \psi_{xt} + i(3\xi_0^2 - V)\psi_x + (\xi_0^3 - 3\xi_0 V)\psi + 3\xi_0\psi_{yy} + i\xi_0\psi_t = 0. \quad (21)$$

Absorbing boundary conditions on the west, north and south boundaries can also be obtained through using $(1, 1)$-Padé approximations to ξ^2 centered at $-\xi_0$, to η^2 centered at η_0, and to η^2 centered at $-\eta_0$, respectively, which are

$$\Gamma_w : \quad i\psi_{xyy} - \psi_{xt} + i(3\xi_0^2 - V)\psi_x - (\xi_0^3 - 3\xi_0 V)\psi - 3\xi_0\psi_{yy} - i\xi_0\psi_t = 0, \quad (22)$$

$$\Gamma_n : \quad i\psi_{xxy} - \psi_{yt} + i(3\eta_0^2 - V)\psi_y + (\eta_0^3 - 3\eta_0 V)\psi + 3\eta_0\psi_{xx} + i\psi_t = 0, \quad (23)$$

$$\Gamma_s : \quad i\psi_{xxy} - \psi_{yt} + i(3\eta_0^2 - V)\psi_y - (\eta_0^3 - 3\eta_0 V)\psi - 3\eta_0\psi_{xx} - i\psi_t = 0, \quad (24)$$

with η_0 a positive constant as ξ_0.

Now let us look at the formula at the north east corner $(x, y) = (L, L)$. We can also approximate the two dimensional dispersion relation (18) in the quarter $\{(\xi, \eta) : \xi > 0, \eta > 0\}$ using $(1,1)-$Padé to both ξ^2 and η^2 with the corresponding centered point (ξ_0, η_0) to obtain

$$\xi_0^2 \frac{-3\xi + \xi_0}{\xi - 3\xi_0} + \eta_0^2 \frac{-3\eta + \eta_0}{\eta - 3\eta_0} = \omega - V \qquad (25)$$

Then after multiplying $(\xi - 3\xi_0)(\eta - 3\eta_0)$ in both sides, we have,

$$-\omega\xi\eta + 3\xi_0\omega\eta + 3\eta_0\omega\xi + (V - 3\xi_0^2 - 3\eta_0^2)\xi\eta - 9\xi_0\eta_0\omega + (\xi_0^3 + 9\xi_0\eta_0^2 - 3\xi_0 V)\eta$$
$$+ (\eta_0^3 + 9\xi_0^2\eta_0 - 3\eta_0 V)\xi + (9\xi_0\eta_0 V - 3\xi_0^3\eta_0 - 3\eta_0^3\xi_0) = 0. \qquad (26)$$

Then performing the inverse transform to physical space yields the ABC(1,1) at the corner point,

$$i\psi_{xyt} + 3\xi_0\psi_{yt} + 3\eta_0\psi_{xt} + (3\xi_0^2 + 3\eta_0^2 - V)\psi_{xy} - 9i\xi_0\eta_0\psi_t - i(\xi_0^3 + 9\xi_0\eta_0^2 - 3\xi_0 V)\psi_y$$
$$- i(\eta_0^3 + 9\xi_0^2\eta_0 - 3\eta_0 V)\psi_x + (9\xi_0\eta_0 V - 3\xi_0^3\eta_0 - 3\eta_0^3\xi_0)\psi = 0. \qquad (27)$$

Extension of the adaptive parameter selection for one-dimensional version to multidimensional cases is straightforward. We note that a multidimensional

problem can be split into a series of one-dimensional ones. Thus we can obtain the estimation of the parameters at every boundary grid points by a dimension-by-dimension procedure. For example, in order to compute the wave number on the east boundary, we have the Gabor transform in x direction:

$$\tilde{\psi}(\xi, y, t) = \int_{L-b(y)}^{L} \psi(x, y, t)e^{-i\xi x}dx, \tag{28}$$

where the window length is a function of y. The parameter $\xi_0(y)$ can then be determined by using the method in section 2.2.

3 Nonlinear Schrödinger equations

We now consider the nonlinear Schrödinger equation in two dimensions as follows,

$$i\psi_t(x, y, t) = -(\psi_{xx} + \psi_{yy}) + f(|\psi|^2)\psi + V(x, y, t)\psi, \quad (x, y) \in \mathbb{R}^2. \tag{29}$$

We shall extend the previous work of the split local absorbing boundary (SLAB) method [35] in one-dimensional version to solving the two-dimensional case. Denote the approximation of ψ on the grid point (x_ι, y_j, t^n) by $\psi_{\iota j}^n$ for $0 \le \iota \le I$ and $0 \le j \le J$, with $x_\iota = \iota\Delta x$, $y_j = j\Delta y$, $t^n = n\Delta t$, and $x_I = y_J = L$. Let us first describe the finite difference scheme for the Eq. (29) in the interior domain $(0, L)^2$, which will be connected with the discretization on the artificial boundaries.

3.1 Semi-implicit interior scheme

In our previous work in one dimension [35], the full-implicit Crank-Nicholson scheme, which is unconditionally stable, was used. However, one has to solve the nonlinear algebraic system iteratively at each time step. It is time consuming in particular for the two dimensional case. In order to avoid the iterative process, we use the following semi-implicit scheme [37], which was shown efficient and robust in comparison with various difference schemes for solving nonlinear Schrödinger equations [38],

$$i\frac{\psi_{\iota j}^{n+1} - \psi_{\iota j}^n}{\Delta t} = -(D_x^+ D_x^- + D_y^+ D_y^-)\frac{\psi_{\iota j}^{n+1} + \psi_{\iota j}^n}{2} + [\frac{3}{2}f(|u_{\iota j}^n|^2) - \frac{1}{2}f(|u_{\iota j}^{n-1}|^2) + V_{\iota j}]\frac{\psi_{\iota j}^{n+1} + \psi_{\iota j}^n}{2},$$
$$\tag{30}$$

where D^+ and D^- represent the forward and backward differences, respectively. This is a five-points scheme and its truncation error is order $O(\Delta t^2 +$

$\Delta x^2 + \Delta y^2$) as that of the Crank-Nicholson scheme. However, since the non-linear term is approximated by the known variables through an extrapolation formula, we need only to solve a linear algebraic system at each time step.

3.2 Numerical approximation on the artificial boundary

We have obtained the discrete scheme by formula (30) in the interior point (x_ι, y_j) for $1 \leq \iota \leq I - 1$ and $1 \leq j \leq J - 1$. Now we concentrate on the boundary conditions, in which we shall perform the local time-splitting procedure. The basic idea of the SLAB method is to split the original equation in several subproblems which are easy to be handled, and then solve them alternatively in a small time step Δt. Consider a standard splitting for Eq. (29) in the vicinity of the artificial boundary to a nonlinear subproblem

$$i\psi_t = f(|\psi|^2)\psi, \tag{31}$$

and a linear subproblem

$$i\psi_t = -(\psi_{xx} + \psi_{yy}) + V\psi. \tag{32}$$

We carry out the splitting on boundary points $\{x_\alpha, y_\beta\}$ for

$$\alpha \in \{0, 1, I - 1, I\}, \quad \text{and} \quad \beta \in \{0, 1, J - 1, J\}.$$

Following [39], in the nonlinear step, we have an approximate solver for explicitly discretizing the ODE (31)

$$\psi^*_{\alpha,\beta} = e^{-if(|\psi^n_{\alpha,\beta}|^2)\Delta t}\psi^n_{\alpha,\beta}, \tag{33}$$

which keeps ψ invariant, and does not require any boundary condition. Noting the next step for the time-splitting procedure is to integrate a linear subproblem (32), we impose here the local absorbing boundary condition discussed in Section 2. For example, using formulae (21), (27) and their corresponding formulae on every boundaries and corners, we obtain the full scheme of the problem by approximating them with finite difference expressions. Here the discrete forms of the terms in the east boundary condition (21) are

$$\psi_x = D_x^- \frac{\psi^{n+1}_{I,j} + \psi^*_{I,j}}{2}, \qquad \psi = S_x^- \frac{\psi^{n+1}_{I,j} + \psi^*_{I,j}}{2}, \tag{34}$$

$$\psi_{xt} = D_x^- \frac{\psi^{n+1}_{I,j} - \psi^*_{I,j}}{\Delta t}, \qquad \psi_t = S_x^- \frac{\psi^{n+1}_{I,j} - \psi^*_{I,j}}{\Delta t}, \tag{35}$$

$$\psi_{xyy} = D_x^- D_y^+ D_y^- \frac{\psi^{n+1}_{I,j} + \psi^*_{I,j}}{2}, \psi_{yy} = S_x^- D_y^+ D_y^- \frac{\psi^{n+1}_{I,j} + \psi^*_{I,j}}{2}, \tag{36}$$

with S^- the backward sum, for example,

$$S_x^- \psi_{I,j}^* = \frac{1}{2}(\psi_{I-1,j}^* + \psi_{I,j}^*);$$

and the discrete forms of the terms in the corner boundary condition (27) are

$$\psi_{xyt} = D_x^- D_y^- \frac{\psi_{I,J}^{n+1} - \psi_{I,J}^*}{\Delta t}, \psi_{xy} = D_x^- D_y^- \frac{\psi_{I,J}^{n+1} + \psi_{I,J}^*}{2}, \tag{37}$$

$$\psi_{yt} = S_x^- D_y^- \frac{\psi_{I,J}^{n+1} - \psi_{I,J}^*}{\Delta t}, \ \psi_y = S_x^- D_y^- \frac{\psi_{I,J}^{n+1} + \psi_{I,J}^*}{2}, \tag{38}$$

$$\psi_{xt} = D_x^- S_y^- \frac{\psi_{I,J}^{n+1} - \psi_{I,J}^*}{\Delta t}, \ \psi_x = D_x^- S_y^- \frac{\psi_{I,J}^{n+1} + \psi_{I,J}^*}{2}, \tag{39}$$

$$\psi_t = S_x^- S_y^- \frac{\psi_{I,J}^{n+1} - \psi_{I,J}^*}{\Delta t}, \ \ \psi = S_x^- S_y^- \frac{\psi_{I,J}^{n+1} + \psi_{I,J}^*}{2}. \tag{40}$$

Similar discretizations can be used for the other three boundaries and the other three corners. Thus we obtain the full-discrete scheme for the nonlinear Schrödinger equation (29) in two dimensions, which yields a linear algebraic system at each time steps.

Remark 3. Near the artificial boundaries, the truncation error of accuracy is $(\Delta x^2 + \Delta y^2 + \Delta t)$ because we only adopt the first-order splitting. In order to improve the accuracy of time-splitting to higher order, such as using the Strang splitting [40], we will obtain a nonlinear algebraic system which have to be solved through the iterate approach as discussed in Ref. [35].

4   Numerical examples

We test our absorbing boundary conditions given in the previous sections for the nonlinear Schrödinger equation. In particular, we test the strategy of adaptive parameter selection in the one-dimensional case. Based on its outstanding performance in one dimension, two-dimensional example of extensions is also given.

Example 1. We are going to test the performance of the adaptive parameter selection for absorbing boundary conditions by solving the cubic nonlinear Schrödinger equation in one dimension

$$i\psi_t = -\psi_{xx} + g|\psi|^2\psi + V\psi, \tag{41}$$

where g is a real constant and $V \equiv 0$. If g is positive, the equation represents repulsive interactions. If g is negative, the equation represents attractive

interactions, and admits bright soliton solution

$$\psi(x,t) = A\sqrt{\frac{-2}{g}}\sec(Ax - 2ABt)e^{iBx+6(A^2-B^2)t} \tag{42}$$

with A, B real parameters related to the amplitude and velocity of the soliton. The numerical scheme is the 1D reduction of 2D version described in Section 3. The first example we consider the case of $g = -2$ and the initial condition

$$\psi(x,t) = \sec(x - 10)e^{2i(x-10)} + \sec(x - 30)e^{5i(x-30)}. \tag{43}$$

It represents two solitons with amplitude 1, located at two isolated centers $x = 10$ and 30 respectively, propagate to the right. Their propagating velocities are double of their wave numbers; that is, 4 and 10, respectively. We compute the solution up to $t^n = 10$ in interval $[0, L]$ for $L = 40$. As in $[22, 24, 35]$, to see the influence of parameter k_0, we evaluate the effectiveness of absorbing boundary conditions by calculating the reflection ratios as follows,

$$r = \sum_{j=0}^{I} |\psi_j^n|^2 / \sum_{j=0}^{I} |\psi_j^0|^2. \tag{44}$$

The ratio r is handy in the measurement of the quality of the ABC. For example, $r = 0$ reflects that the solitons have passed through the boundary completely; whereas $r = 1$ indicates the waves are completely reflected into the interior domain by the artificial boundaries. At the left boundary $x = 0$, we set $k_0 = 0$ since there is no left-going wave. We also hope the reflected waves from the right boundary can also be reflected by the left boundary, therefore the reflection ratios of absorbing boundary conditions at the right boundary can be correctly calculated. We show numerical results in Table 1 for different p in (16) and different transforms, in which we also illustrate L_1-errors defined by

$$E_1 = \frac{1}{I+1} \sum_{j=0}^{I} |\psi_j^n - \psi(x_j, t^n)|. \tag{45}$$

Here and hereafter, the time steps Δt are taken to be $\Delta t = \Delta x^2$. It is not the restriction of stability, but the requirement for compensating the accuracy since we just use the first-order splitting on the artificial boundaries. For the Gabor transform to pre-estimate the parameter, the window lengths are set to $b = L/4$. We also compare the results in Table 2 without the adaptive parameter selection but fixing the parameter $k_0 = 2$, 3.5 and 5, respectively. It is observed that the weighted wave-number parameter method can well improve numerical accuracy.

There are two time phases in the process for the two solitons hit the right boundary separately. The first phase is for $t \in [0.5, 1.5]$ when the first wave with the wave number 5 transmits the boundary; while the second phase is

12
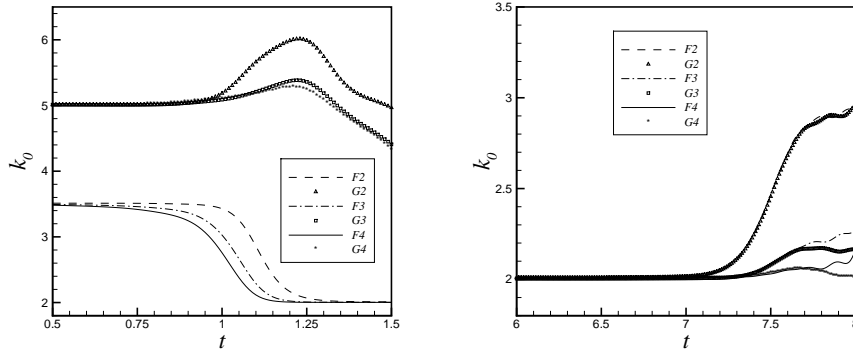
Fig. 1. Weighted wave numbers k_0 as a function of time. Left: the first phase for $t \in [0.5,\ 1.5]$; right: the second phase for $t \in [6,\ 8]$.

for $t \in [6,\ 8]$ when the second wave with the wave number 2 passes through the boundary. In order to see the resultant wave-number parameter of the methods in discussion, we illustrate the wave numbers as a function of time t for two phases in Fig. 1, where we denote the resultant wave number with Fourier transform and p norm by Fp wave number, the results with Gabor transform and p norm by Gp wave number. We see that the parameters with Gabor transform, especially when $p = 4$, response a better information for the solution, which well agrees with the results in Table 1.

In order to see the influence of the window length b, we compute the solution for different lengths in Table 3 with a fixed p. The window length is in direct proportion to the wave number $b = \beta k_0$, in which k_0 takes the value at time $t = t^{n-1}$ for the calculations at t^n. We see that it is necessary to choose a β larger than 1.

Table 1 L_1-errors E_1 and reflection ratios r for different parameters and grid sizes with adaptive parameter selection.

p	E_1 for $\Delta x = 0.1$		E_1 for $\Delta x = 0.05$		r for $\Delta x = 0.1$		r for $\Delta x = 0.05$	
	Fourier	Gabor	Fourier	Gabor	Fourier	Gabor	Fourier	Gabor
1	1.62d-2	1.79d-2	3.28d-2	3.47d-2	7.43d-3	7.63d-3	2.87d-2	2.94d-2
2	5.12d-3	2.72d-3	4.51d-3	2.62d-3	3.79d-4	1.65d-4	3.23d-4	1.70d-4
3	5.29d-3	1.93d-3	4.69d-3	1.54d-3	3.66d-4	7.32d-5	2.99d-4	4.48d-5
4	5.27d-3	1.93d-3	5.01d-3	1.56d-3	3.76d-4	7.14d-5	3.45d-4	4.21d-5
5	5.07d-3	1.95d-3	5.07d-3	1.59d-3	3.70d-4	7.23d-5	3.70d-4	4.49d-5

Table 2 L_1-errors E_1 and reflection ratios r for different parameters and grid sizes without adaptivity.

k_0	E_1		r	
	$\Delta x = 0.1$	0.05	0.1	0.05
2	3.22d-3	3.26d-3	2.00d-4	1.73d-4
3.5	5.33d-3	4.98d-3	8.58d-4	7.89d-4
5	1.26d-2	1.23d-2	4.81d-3	4.60d-3

Table 3 L_1-errors E_1 and reflection ratios r for different window lengths determined adaptively as $b = \beta k_0$. $p = 4$.

β	E_1		r	
	$\Delta x = 0.1$	0.05	0.1	0.05
0.5	7.71d-3	2.10e-3	1.73e-3	1.23e-4
1	1.91d-3	1.57d-3	7.35d-5	4.37d-5
2	1.92d-3	1.55d-3	6.93d-5	4.10d-5
3	1.92d-3	1.53d-3	7.02d-5	3.98d-5
4	1.93d-3	1.54d-3	7.09d-5	4.02d-5

Example 2. We then consider a nonlinear wave with repulsive interaction ($g = 2$ in Eq. (41)). The initial data and potential function are taken to be Gaussian pulses

$$\psi(x,0) = e^{-0.1(x-x_0)^2} \text{ and } V(x) = e^{-0.5(x-x_0)^2}, \tag{46}$$

with $x_0 = 15$. This has been an example in [35] used to model expansion of a Bose-Einstein condensate which is composed of waves with different group velocities. The frequency context at the boundaries is depending on the temporal evolution. In [35], the authors obtained the results under different wavenumber parameters which are independent of time t. It was illustrated that a very bad result appeared if we cannot choose a suitable k_0. Therefore, it is necessary to capture this parameter adaptively in order to minimize the nonphysical reflection.

In the calculation, $L = 30$, $\Delta x = 0.1$, and $\Delta t = 0.01$ are chosen. The numerical results with the same mesh sizes by using the proposed ABC in a large domain $[-15, 45]$ are taken to be a reference solution which is regarded as the "exact" solution, since the analytic solution is unknown. Fig. 2 shows the motion of

14
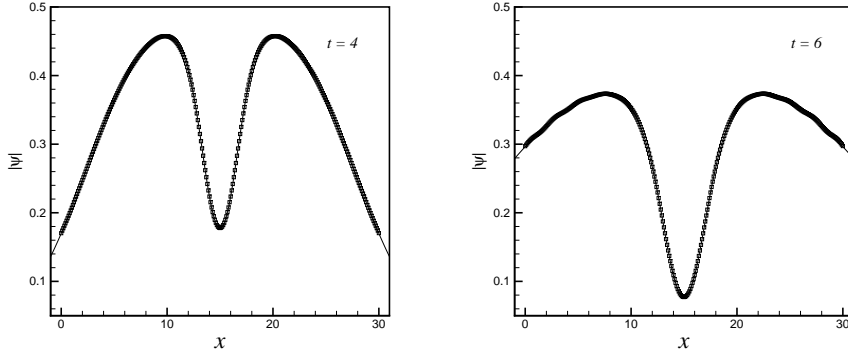
Fig. 2. The $|\psi|$ solutions at time $t = 4$ and 6.
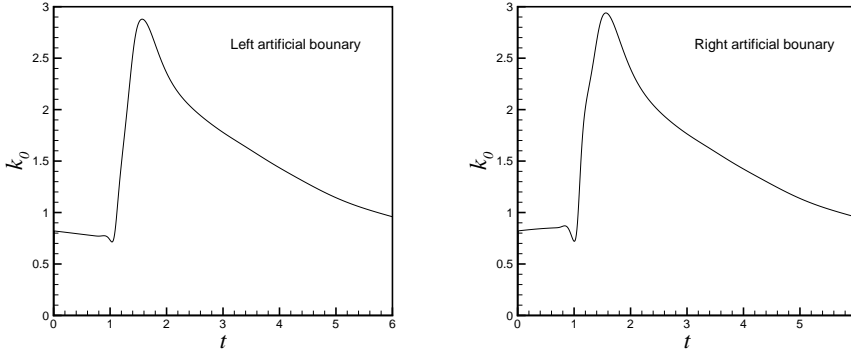
Fig. 3. The wave numbers k_0 as functions of time t.

the wave with the ABCs at time $t = 4$ and 6, in which we take $p = 4$ and the window length of Gabor transform $b = L/4$. It is illustrated that the reflected wave is very small when the waves hit the boundaries under our adaptive parameter selection strategy. We also show the wave-number parameters at both boundaries as functions of time in Fig. 3, in which we see that the wave numbers decay with time after the waves reach artificial boundaries.

Example 3. This is a two-dimensional example for Eq. (29) with cubic non-linearity $f(|\psi|^2) = -|\psi|^2$ in homogeneous media; i.e., the potential $V \equiv 0$. We consider the temporal evolution of an initial packet of the wave centered at $(x, \ y) = (5, \ 5)$

$$\psi(x, y, 0) = \sqrt{2}e^{(x-5)^2+(y-5)^2}e^{2i(x+y-10)}. \tag{47}$$

The wave packet moves along the northeast direction and impinges on the artificial boundaries Γ_e and Γ_n. At the same time, the amplitude of the wave

15
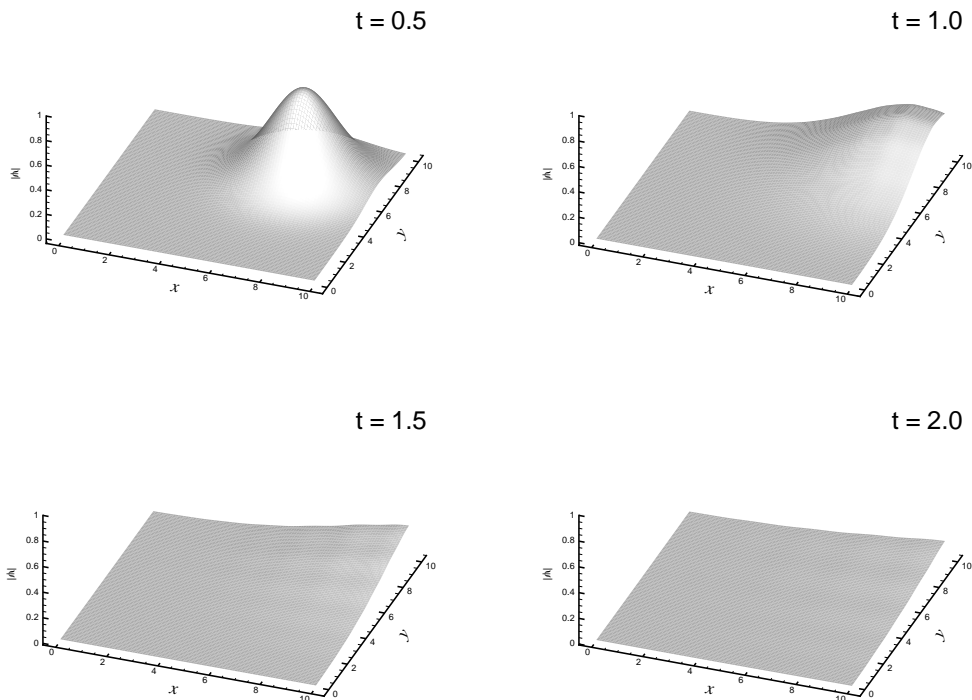
Fig. 4. Numerical solutions of $|\psi|$ under the mesh size $\Delta x = \Delta y = 0.05$ and $\Delta t = 0.0025$ at time $t = 0.5,\ 1,\ 1.5$ and 2.

packet deceases with time due to the expansion effect. In the calculations, we set the computational domain be $[0, L]^2$ for $L = 10$. We also set $p = 4$ and the window length of Gabor tranform $b = L/4$. We show numerical solutions of $|\psi|$ at time $t = 0.5,\ 1,\ 1.5$ and 2 in Fig. 4 for $h = \Delta x = \Delta y = 0.05$ and $\Delta t = h^2$. We see the wave can be well absorbed with only minor reflections. In order to see the errors, we take the numerical result in a large domain $[0, 20]^2$ with $h = 0.05$ to be a reference solution. In Fig. 5, we plot the temporal evolution of the solutions and their errors for different mesh sizes at positions $(x, y) = (10,\ 10)$ and $(10, 5)$. These results illustrate that the discussed method can also works well for the two-dimensional problem.

5 Concluding remarks

We develop an efficient adaptive parameter approach for absorbing boundary conditions of Schrödinger-type equations. This approach is coupled with the

16
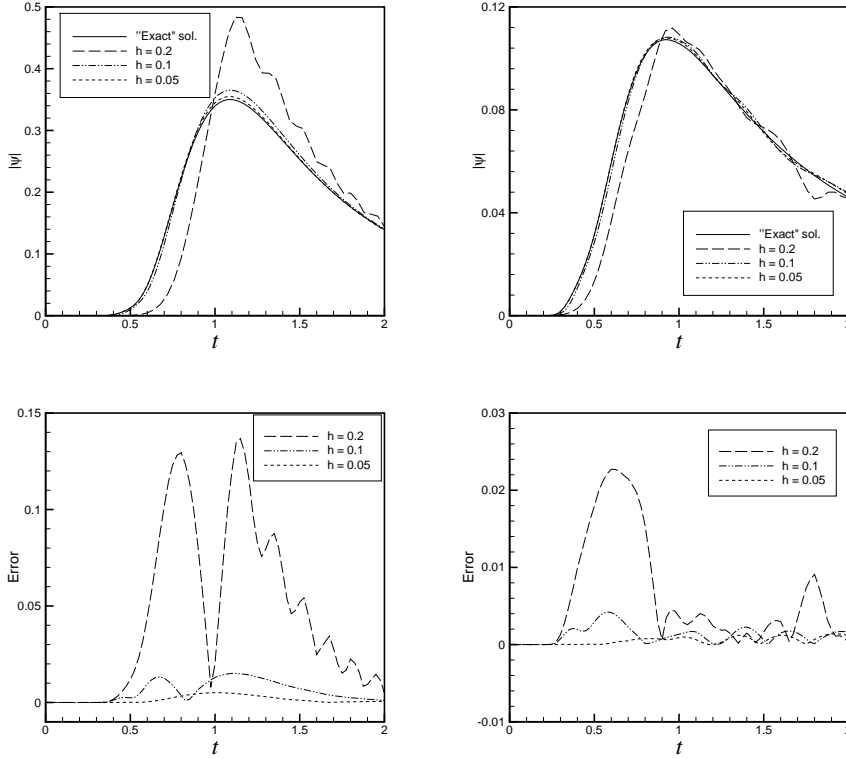
Fig. 5. Temporal evolutions and errors of $|\psi|$ at positions: $(x, y) = (10, 10)$ (Left), and $(x, y) = (10, 5)$ (Right). The "exact" solution is computed in a large domain $[0, 20]^2$ with the mesh size $h = 0.05$

local time-splitting method to constitute a complete procedure for nonlinear problems. We also introduce an extension to deal with absorbing boundary conditions for multidimensional nonlinear Schrödinger equations. Numerical examples are performed to show the attractive features of the approach under consideration. Related further work includes the stability and error analysis of the proposed approach and further extension to more complicated initial-boundary value problems. Another problem is induced by the complexity of nonlinear mechanics. In some situations, the outgoing waves will return to the interior domain due to their interactions of nonlinear packets. This open problem is still unsolved in this paper and we leave for further consideration.

Acknowledgments

References

[1] C. Sulem and P.L. Sulem. *The Nonlinear Schrodinger Equation: Self-Focusing and Wave Collapse.* Springer, 1999.

[2] G.P. Agrawal. *Nonlinear fiber optics, 3rd Ed.* Academic Press, San Diego, 2001.

[3] D. Givoli. *Numerical Methods for Problems in Infinite Domains.* Elsevier, Amsterdam, 1992.

[4] S. V. Tsynkov. Numerical solution of problems on unbounded domains. a review. *Appl. Numer. Math.*, 27:465–532, 1998.

[5] T. Hagstrom. Radiation boundary conditions for the numerical simulation of waves. *Acta Numerica*, pages 47–106, 1999.

[6] H. Han. The artificial boundary method – numerical solutions of partial differential equations on unbounded domains. In T. Li and P. Zhang, editors, *Frontiers and Prospects of Contemporary Applied Mathematics*, pages 33–58. Higher Education Press and World Scientific, 2006.

[7] B. Engquist and A. Majda. Absorbing boundary conditions for the numerical simulation of waves. *Math. Comput.*, 31:629–651, 1977.

[8] R.L. Higdon. Absorbing boundary conditions for difference approximations to the multi-dimensional wave equation. *Math. Comput.*, 47:437–459, 1986.

[9] H.D. Han and X.N. Wu. Approximation of infinite boundary condition and its applications to finite element methods. *J. Comput. Math.*, 3:179–192, 1985.

[10] D.H. Yu. Approximation of boundary conditions at infinity for a harmonic equation. *J. Comput. Math.*, 3:219–227, 1985.

[11] L. Halpern and J. Rauch. Absorbing boundary conditions for diffusion equations. *Numer. Math.*, 71:185–224, 1995.

[12] H. Han and Z. Huang. Exact and approximating boundary conditions for the parabolic problems on unbounded domains. *Comput. Math. Appl.*, 44:655–666, 2002.

[13] F. Schmidt and D. Yevick. Discrete transparent boundary conditions for Schrödinger-type equations. *J. Comput. Phys.*, 134:96–107, 1997.

[14] A. Arnold. Numerically absorbing boundary conditions for quantum evolution equations. *VSLI Design*, 6:313–319, 1998.

[15] A. Arnold, M. Ehrhardt, and I. Sofronov. Discrete transparent boundary conditions for the Schrödinger equation: Fast calculation, approximation, and stability. *Commun. Math. Sci.*, 1:501–556, 2003.

[16] X. Antoine and C. Besse. Unconditionally stable discretization schemes of non-reflecting boundary conditions for the one-dimensional Schrödinger equation. *J. Comput. Phys.*, 188:157–175, 2003.

[17] H. Han and Z. Huang. Exact artificial boundary conditions for Schrödinger equation in R^2. *Commun. Math. Sci.*, 2:79–94, 2004.

[18] Z. Z. Sun and X. Wu. The stability and convergence of a difference scheme for the Schrödinger equation on an infinite domain by using artificial boundary conditions. *J. Comput. Phys.*, 214:209–223, 2006.

[19] H. Han, J. Jin, and X. Wu. A finite-difference method for the one-dimensional time-dependent Schrödinger equation on unbounded domain. *Comput. Math. Appl.*, 50:1345–1362, 2005.

[20] S. D. Jiang and L. Greengard. Fast evalution of nonreflecting boundary conditions for the Schrödinger equation in one dimension. *Comput. Math. Appl.*, 47:955–966, 2004.

[21] T. Shibata. Absorbing boundary conditions for the finite-difference time-domain calculation of the one dimensional Schrödinger equation. *Phys. Rev. B*, 43:6760, 1991.

[22] J.-P. Kuska. Absorbing boundary conditions for the Schrödinger equation on finite intervals. *Phys. Rev. B*, 46:5000, 1992.

[23] L. Di Menza. Transparent and absorbing boundary conditions for the Schrödinger equation in a bounded domain. *Numer. Funct. Anal. Optim.*, 18:759–775, 1997.

[24] T. Fevens and H. Jiang. Absorbing boundary conditions for the Schrödinger equation. *SIAM J. Sci. Comput.*, 21:255–282, 1999.

[25] I. Alonso-Mallo and N. Reguera. Weak ill-posedness of spatial discretizations of absorbing boundary conditions for Schrödinger-type equations. *SIAM J. Numer. Anal.*, 40:134–158, 2002.

[26] J. Szeftel. Design of absorbing boundary conditions for Schrödinger equations in R^d. *SIAM J. Numer. Anal.*, 42:1527–1551, 2004.

[27] T. Hagstrom and H.B. Keller. Asymptotic boundary conditions and numerical methods for nonlinear elliptic problems on unbounded domains. *Math. Comput.*, 48:449–470, 1987.

[28] H.D. Han, X.N. Wu, and Z.L. Xu. Artificial boundary method for Burgers' equation using nonlinear boundary conditions. *J. Comput. Math.*, 24:295–304, 2006.

[29] Z. Xu, H. Han, and X. Wu. Numerical method for the deterministic Kardar-Parisi-Zhang equation in unbounded domains. *Commun. Comput. Phys.*, 1:481–495, 2006.

[30] C. Zheng. Exact nonreflecting boundary conditions for one-dimensional cubic nonlinear Schrödinger equations. *J. Comput. Phys.*, 215:552–565, 2006.

[31] X. Antoine, C. Besse, and S. Descombes. Artificial boundary conditions for one-dimensional cubic nonlinear Schrödinger equations. *SIAM J. Numer. Anal.*, 43:2272–2293, 2006.

[32] J. Szeftel. Absorbing boundary conditions for nonlinear scalar partial differential equations. *Comput. Methods Appl. Mech. Engrg.*, 195:3760–3775, 2006.

[33] J. Szeftel. Absorbing boundary conditions for one-dimensional nonlinear Schrödinger equations. *Numer. Math.*, 104:103–127, 2006.

[34] C. Farrell and U. Leonhardt. The perfectly matched layer in numerical simulations of nonlinear and matter waves. *J. Opt. B: Quantum Semiclass. Opt.*, 7:1–4, 2005.

[35] Z. Xu and H. Han. Absorbing boundary conditions for nonlinear Schrödinger equations. *Phys. Rev. E*, 74:037704, 2006.

[36] D. Gabor. Theory of communication. *J. Inst. Elect. Eng. (London)*, 93:429–457, 1946.

[37] P.L. Sulem, C. Sulem, and A. Patera. Numerical simulation of singular solutions to the two-dimensional cubic Schrödinger equation. *Commum. Pure Appl. Math.*, 37:755–778, 1984.

[38] Q. Chang, E. Jia, and W. Sun. Difference schemes for solving the generalized nonlinear Schrödinger equation. *J. Comput. Phys.*, 148:397–415, 1999.

[39] W. Bao, S. Jin, and P.A. Markowich. Numerical study of time-splitting spectral discretizations of nonlinear Schrödinger equations in the semiclassical regimes. *SIAM J. Sci. Comput.*, 25:27–64, 2003.

[40] G. Strang. On the constrction and comparison of difference schemes. *SIAM J. Numer. Anal.*, 5:506–517, 1968.